Frontiers in Computing and Intelligent Systems
ISSN: 2832-6024 | Vol. 14, No. 2, 2025

High-Resolution Inversion of Seismic Stress Fields and Dynamic Hazard Analysis via Adaptive Physics-Informed Neural Networks and NGL GNSS Data Fusion

Ming Chen

Bishop Alemany High School, Los Angeles, California, USA

Abstract: Proper inversion of the seismic stress field is essential in the studies of fault activity as well as earthquake hazards. The simplified physical models and paucity of observations constrain the traditional methods. The proposed paper offers a new framework, where ANN is Adaptive Physics-Informed Neural Network (Adaptive-PINN), which combines high-precision GNSS surface velocity field values in the Nevada Geodetic Laboratory (NGL) and in its result, achieves high-resolution inversion of the crustal stress field and dynamic hazard analysis. It uses deep neural networks to build a nonlinear model of geographic coordinates to stress-field parameters and applies physical plausibility through embedded constraints (e.g., stress equilibrium equations and constitutive relations). The adaptive mechanism that is proposed uses the weights of the losses dynamically in such a way that they place more emphasis on regions with large physical residuals, which has a substantial effect on the interpretability and convergence ability. An example of a case study on how global GNSS velocity fields can be used to create spatially continuous, high-resolution stress maps and an earthquake hazard index. Conclusions indicate that the technique is effective to not only recreate stress concentrations along established active tectonic belts but also possible high risk zones which has created a potent new resource in the process of earthquake dynamics, as well as disaster risk assessment.

Keywords: Adaptive Physics-Informed Neural Networks; GNSS; Stress-field Inversion; Earthquake Hazard; Deep Learning.

1. Introduction

1.1. Background and Significance

This is the crustal stress state, which is the driving force of earthquake nucleation and occurrence. The accurate description of the spatial distribution, magnitude, and direction of regional stress fields is important in the study of fault behavior, seismic potential, and the prediction of places of strong earthquakes. Direct data on deep crustal stress are very hard to obtain so inversion of indirect measurements (e.g., focal mechanisms, borehole breakout data) is commonly employed, but frequently has low spatial resolution, non-uniform coverage, or is too expensive.

The use of Global Navigation Satellite System (GNSS) observations offers long term three dimensional velocity of the surface of wide regions with high precision. Surface deformation being a straight reaction to stress concentration and adaptation in the crust, GNSS velocity fields make a useful source of data in the inversion of stress fields. Conventional inversion techniques based on either the elastic/viscoelastic dislocation theory or continuum mechanics provides replacements of observation in a set of pre-defined physical models. Although physically interpretable, they are highly sensitive to simplified assumptions (e.g. homogeneous half-space, simple fault geometry), which are difficult to make realistic in terms of their ability to portray realistic heterogeneity and nonlinear rheology.

1.2. Limitations and Challenges

GNSS-based stress inversion presents two fundamental challenges:

(1) Model limitations. Classical physical models also have a tendency to simplify complicated geophysical reality and in most cases, they do not represent well the lithospheric rheology and interaction between the different faults.

(2) Sparsity and ill-posedness of data. The fact that GNSS stations are discrete and uneven makes the reconstruction of a continuous spatial stress field ill-posed hence non-uniqueness and sensitive to measurement noise.

Although deep learning has shown promise in geoscience for learning nonlinear patterns, purely data-driven models often lack physical constraints[1]. This can lead to physically inconsistent results and poor generalization when applied to unseen regions.

1.3. This Study and Contributions

PINNs use the partial differential equations (PDEs) of physical systems[2] in the loss function and combines data-driven and physics-driven learning. We suggest a GNSS-based inversion of seismic stress field by an Adaptive-PINN. Some of the significant contributions are:

Physical limits to a deep degree - Developing an entire chain of inference between GNSS velocities and crustal stress including velocity gradients, strain-rate tensors, stress through linear elasticity of the crust and equilibrium of forces.

High-resolution hazard analysis — Producing continuous hazard maps by deriving a composite index of earthquake hazard based on multi-stress parameters (e.g. shear stress, von Mises stress).

2. Theoretical Background

2.1. GNSS Observations and Crustal Deformation

Processing GNSS observations produces 3-D station coordinate time series, from which we derive velocities in the east (Ve), north (Vn), and up (Vu) directions. In tectonically active areas, long-term deformation signals exceed the background noise, so GNSS is highly effective for tracking

crustal motion. The surface velocity field v(x, y) reflects the integrated surface response to the subsurface stress field σ(x, y, z).

2.2. Continuum Mechanics and Stress Inversion

In the continuum mechanics system, the stress field is constrained by the static force-balance (including the body forces). The equations of stress equilibrium when applied in two dimensions are mathematically stated as:

$$\begin{aligned} \frac{\partial \sigma_{xx}}{\partial x} + \frac{\partial \sigma_{xy}}{\partial y} &= 0, \\ \frac{\partial \sigma_{yx}}{\partial x} + \frac{\partial \sigma_{yy}}{\partial y} &= 0 , \end{aligned} \tag{1}$$

where σ_{ij} are components of the Cauchy stress tensor (with $\sigma_{xy} = \sigma_{yx}$). By linking GNSS-derived surface strain rates to stress via constitutive relations, one can invert for a stress field consistent with equilibrium. In continuum mechanics, spatial velocity gradients produce strain-rate components. Specifically, the infinitesimal strain-rate tensor ε is given by:

$$\epsilon_{ij} = \frac{1}{2}\left(\frac{\partial v_i}{\partial x_j} + \frac{\partial v_j}{\partial x_i}\right) , \tag{2}$$

where v_i are components of the velocity field (e.g., $v_1 = V_e$, $v_2 = V_n$ in the horizontal plane). Assuming an isotropic linear elastic constitutive model (Hooke's law), stress is related to strain by:

$$\sigma_{ij} = \lambda\, \delta_{ij}\, \epsilon_{kk} + 2\,\mu\, \epsilon_{ij} , \tag{3}$$

where λ and μ are Lamé parameters (material constants). The combination of the equilibrium equations and constitutive law (with strain derived from GNSS velocities) provides a physically constrained basis for stress-field inversion[3].

3. Adaptive-PINN for Seismic Stress-Field Inversion

3.1. Network Architecture

The proposed SeismicAdaptivePINN model employs a deep fully connected neural network that maps geographic coordinates to target variables. Inputs comprise normalized latitude and longitude; the network consists of 6 hidden layers with 64 neurons each and Tanh activations. Outputs include GNSS-derived features (e.g., V_e, V_n, speed magnitude, direction, and estimated strain rates) used for subsequent stress computation.

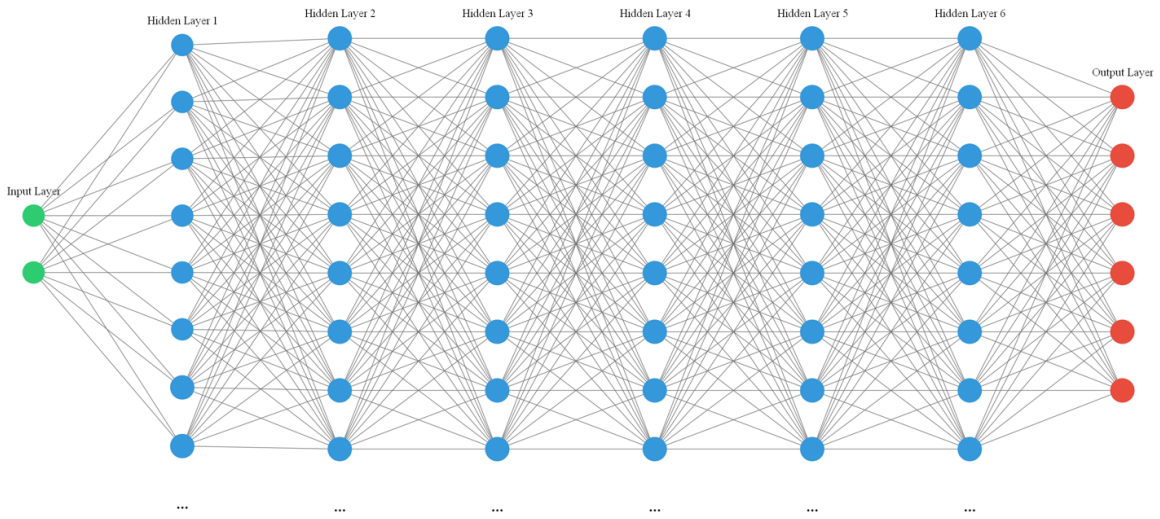

Figure 1. Schematic of the Adaptive-PINN architecture. The model consists of an input layer taking spatial coordinates, followed by 6 hidden layers with 64 neurons each, and an output layer producing six GNSS-derived features (velocity components, magnitude, azimuth, strain rates etc). Tanh activations are applied throughout the hidden layers

The proposed SeismicAdaptivePINN integrates a lightweight, parallel adaptive weighting sub-network[4]. Given coordinates as input, this sub-network predicts a scalar weight (normalized via a Sigmoid function) to amplify loss contributions in locations with larger physical residuals, thereby guiding training attention to physically inconsistent regions.

3.2. Embedded Physical Constraints

Physical constraints are encoded in a physics-based loss term, $L_{physics}$. We enforce that the model's predictions satisfy the stress equilibrium (force-balance) equations as closely as possible. Automatic differentiation is used to compute spatial gradients of the predicted velocity field, enabling construction of strain-rate tensors, stress via linear elasticity, and the residuals of the equilibrium equations (i.e., the degree to which force-balance is violated). The physics loss is defined as:

$$L_{\text{physics}} = \frac{1}{N_p}\sum_{i=1}^{N_p} w\,(\mathbf{x}_i)\ \|\ R(\mathbf{x}_i)\ \|^2 , \tag{4}$$

where the sum is over N_p collocation points in the domain. Here, R(x) is the vector of PDE residuals (i.e., the left-hand side of the equilibrium equations above), and w(x) ∈ (0, 1) is

a spatial weighting factor that modulates the loss contribution at each location x.

In the Adaptive-PINN, w(x) is predicted by an adaptive sub-network to emphasize regions with larger physical residuals. For example, the weight function can be modeled as:

$$w(\mathbf{x}) = \sigma\big(h_\theta(\mathbf{x})\big), \tag{5}$$

where h_θ is a trainable function (a small neural network), and σ is the Sigmoid activation function that maps outputs to the interval (0, 1).

Under a residual-based weighting scheme, points that poorly satisfy the physical constraints (e.g., force balance) receive a larger penalty[5]. This directs training toward reducing those violations.

3.3. Loss and Training Strategy

The total loss function combines both the data-fitting and physics-based penalty terms, each with appropriate weighting. Specifically, the overall PINN loss, L_{total}, is formulated as a weighted sum of the data misfit loss L_{data}—which quantifies the error between predicted and observed GNSS quantities—and the physics loss $L_{physics}$:

$$L_{\text{total}} = \lambda_{\text{data}} L_{\text{data}} + \lambda_{\text{phys}} L_{\text{physics}}, \tag{6}$$

where λ_{data} and λ_{phys} are weighting coefficients. In our Adaptive-PINN framework, these coefficients can be treated as trainable or dynamically adjusted parameters.

Because it prevents one loss component from dominating the optimization, this adaptive strategy yields faster convergence[6], more stable late-stage training, and closer adherence to physical laws. We train a baseline and an adaptive model side by side, usually with SGD (or a variant), and stop when the overall and component losses converge.

4. Experiments and Results

4.1. Data and Preprocessing

We use GNSS horizontal velocity fields from NGL as inputs to the inversion. Preprocessing involves removing outliers; transforming coordinates and standardizing variables (e.g., z-scaling latitude and longitude to limit scale effects); and constructing features—such as speed magnitude and azimuth from Ve and Vn—to serve as network training targets. These steps yield clean, normalized, and feature-rich data for the Adaptive-PINN models.

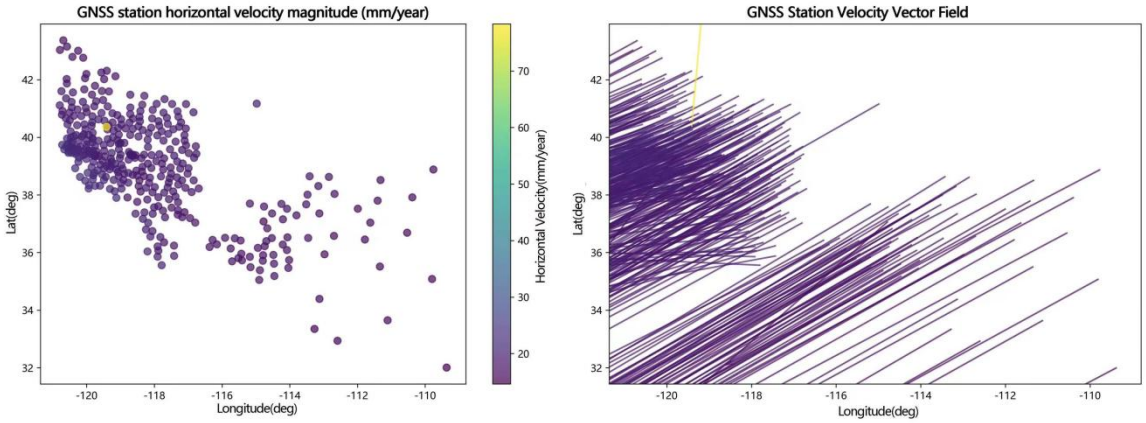

Figure 2. GNSS horizontal velocity magnitude and vector field derived from NGL observations.

The left panel shows the spatial distribution of GNSS station horizontal velocity magnitudes (mm yr^{-1}), while the right panel presents the corresponding horizontal velocity vectors. Arrows indicate both the magnitude and direction of surface motion, with longer arrows representing higher ground velocities associated with active crustal deformation across major fault zones.

4.2. Training and Comparison

Training SeismicAdaptivePINN uses the prepared dataset, with both data and physics losses tracked. Relative to the baseline, the Adaptive-PINN shows a smoother, faster loss decline and reaches a lower final value, indicating better stability and efficiency. The residual-driven weighting, in particular, speeds the drop in physics loss without noticeably harming the data fit. Altogether, Adaptive-PINN converges efficiently and achieves high accuracy on both data and physics constraints [7].

4.3. Stress-Field Inversion Outcomes

After training, we evaluate the model on a regular grid across the study area to obtain stress-field quantities, producing high-resolution parameter maps. The Adaptive-PINN's inferred maximum shear stress shows strong concentrations that trace major active faults; these highs coincide with mapped tectonic belts [8] and zones of historical seismicity, and are sharply resolved. The spatial patterns match regional tectonics and seismicity, indicating that adaptive weighting recovers fine-scale stress structure. By steering attention to difficult areas (e.g., near fault discontinuities), the method yields more detailed and geologically coherent stress inversions.

The total loss (blue), physics loss (red), and data loss (green) are shown across training rounds. The adaptive weighting mechanism effectively reduces physical residuals while stabilizing data fitting, leading to faster and more balanced convergence.

4.4. Earthquake Hazard Analysis

In addition to the stress-field inversion we are able to obtain a composite earthquake hazard index to determine areas of high seismic risk. This is a hazard index, IH, calculated using several stress-related parameters, mostly the maximum shear stress and the von Mises equivalent stress, which is a measure of the accrued tectonic stress as well as the possible failure [9].

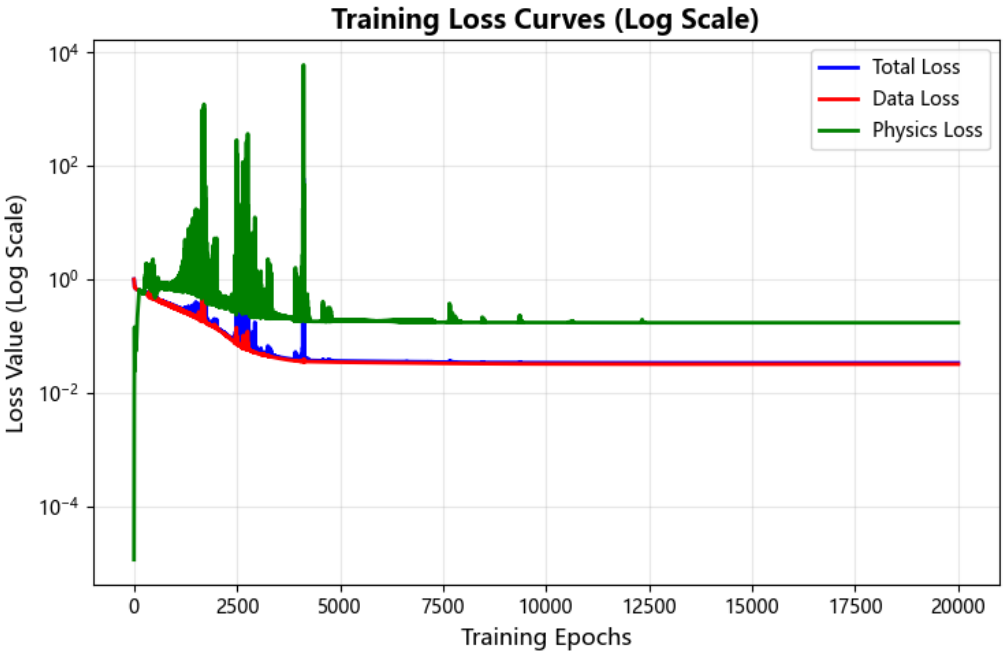

Figure 3. Training loss curve of the Adaptive-PINN model.

First, we obtain the maximum shear stress, τ_{max}, from the stress tensor field (representing the largest shear acting at a point), and the von Mises stress, σ_{vM}, which is a scalar quantity that combines all stress components.

For a two-dimensional stress state, these quantities are defined as:

$$\tau_{\max} = \sqrt{(\frac{\sigma_{xx} - \sigma_{yy}}{2})^2 + \sigma_{xy}^2}\,, \tag{7}$$

$$\sigma_{vM} = \sqrt{\sigma_{xx}^2 + \sigma_{yy}^2 - \sigma_{xx}\,\sigma_{yy} + 3\,\sigma_{xy}^2}\,, \tag{8}$$

where σ_{xx}, σ_{yy}, and σ_{xy} are the components of the predicted stress tensor in the horizontal plane, assuming plane stress conditions.

High values of τ_{max} indicate large differential stress, which promotes shear failure, while high σ_{vM} reflects elevated overall distortional energy.

To construct a unified hazard index, I_H, we normalize both τ_{max} and σ_{vM} by their respective maximum values across the study region and compute their average:

$$I_H(\mathbf{x}) = \frac{1}{2}\left(\frac{\tau_{\max}(\mathbf{x})}{\max(\tau_{\max})} + \frac{\sigma_{vM}(\mathbf{x})}{\max(\sigma_{vM})}\right), \tag{9}$$

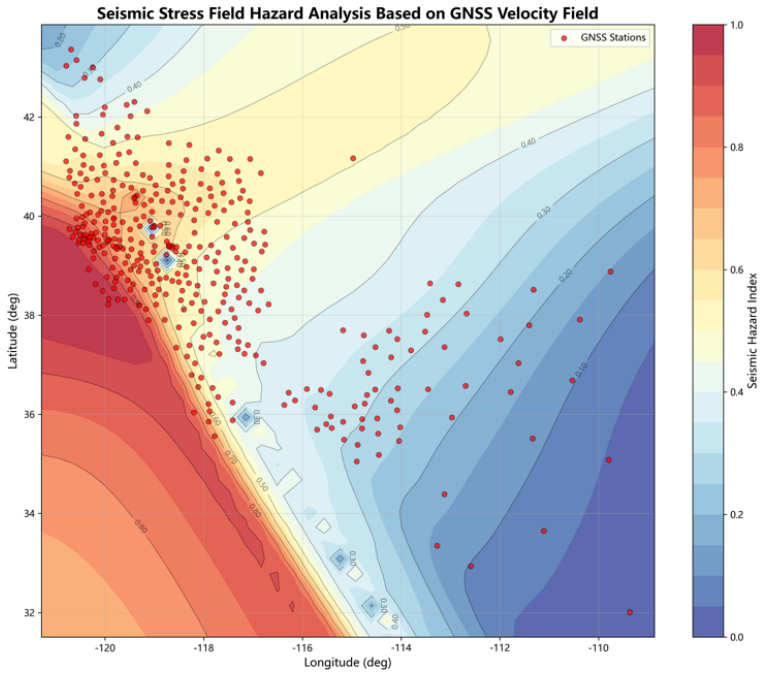

Figure 4. Earthquake hazard index map of the study region, derived from the Adaptive-PINN stress results. Warmer colors (higher index values) indicate zones of greater seismic hazard potential based on the combined stress metrics. The map successfully highlights known active fault regions and also identifies several adjacent areas with elevated hazard, which could be targets for further investigation in seismic risk assessments

which yields a dimensionless index ranging from 0 (lowest hazard) to 1 (highest hazard) in the study area. The resulting hazard map highlights regions that not only correspond well with known seismically active zones (high hazard index along major faults and earthquake-prone areas) but also reveals additional areas that may warrant attention due to elevated model-predicted stress levels.

5. Discussion and Conclusion

5.1. Discussion

The proposed Adaptive-PINN approach tightly integrates GNSS observations with solid mechanics constraints, producing physically grounded, high-resolution stress fields. The model shows superior generalization compared to purely data-driven models, since it is guided by physical laws and thus less likely to produce non-physical results. Moreover, it exhibits a weaker dependence on simplifying assumptions than classical inversion methods. The adaptive weighting mechanism effectively accelerates optimization and boosts accuracy in regions where constraints are challenging to satisfy (e.g., near fault discontinuities or in heterogeneous crustal regions), by directing learning effort to those critical areas[10].

However, the present study assumes a static, quasi-static scenario with linear elasticity; thus, viscoelastic effects, non-linear material behavior, and time-dependent stress changes are not captured. Additionally, the Adaptive-PINN's performance is influenced by the selection of collocation points and the design of the weighting sub-network. In future work, we plan to incorporate more sophisticated rheological models (e.g., non-linear or plastic constitutive laws) and extend the framework to include temporal evolution (time-dependent stress accumulation and release). Further integration of multi-source data (e.g., seismic waveform data, fault geometry, or geological information) could also enhance the model, providing a more comprehensive tool for seismic hazard analysis.

5.2. Conclusion

We developed an Adaptive-PINN-based approach for high-resolution inversion of crustal stress fields using NGL GNSS velocity data. By embedding physical laws as soft constraints and employing an adaptive learning mechanism, the method reconstructs detailed, physically consistent regional stress fields from sparse GNSS observations and enables dynamic earthquake hazard assessment. The results demonstrate that this approach can serve as a powerful new computational paradigm for exploring crustal stress states and improving seismic risk evaluation.

References

[1] Schuster, G. T., & Feng, S. (2024). Review of physics-informed machine-learning inversion of geophysical data. Geophysics, 89(6), T337–T391. https://doi.org/10. 1190/geo 2023-0251.1.

[2] Raissi, M., Perdikaris, P., & Karniadakis, G. E. (2019). Physics-informed neural networks: A deep learning framework for solving forward and inverse problems involving nonlinear partial differential equations. Journal of Computational Physics, 378, 686–707. https://doi.org/10.1016/j.jcp.2018.10.045.

[3] Okazaki, T., Ito, T., Hirahara, K., Ueda, N., & Fukahata, Y. (2022). Physics-informed deep learning approach for modeling crustal deformation. Nature Communications, 13, 7092. https://doi.org/10.1038/s41467-022-34639-1.

[4] Poulet, T., & Behnoudfar, P. (2023). Physics-informed neural network reconciles Australian displacements and tectonic stresses. Scientific Reports, 13, 23095. https://doi.org/ 10. 1038/ s41598-023-49494-6.

[5] Wang, T., Liu, G., Li, E., & Xu, X. (2025). Adaptive deep physics-informed neural network with dual-nested activation for solving complex partial differential equations. Computer Methods in Applied Mechanics and Engineering, 444, Article 118125. https://doi.org/10.1016/j.cma.2025.118125.

[6] Subramanian, S., Kirby, R. M., Mahoney, M. W., & Gholami, A. (2022). Adaptive self-supervision algorithms for physics-informed neural networks. arXiv preprint arXiv:2207.04084. https://arxiv.org/abs/2207.04084.

[7] Fukushima, R., Kano, M., Hirahara, K., Ohtani, M., Im, K., & Avouac, J.-P. (2025). Physics-informed deep learning for estimating the spatial distribution of frictional parameters in slow slip regions. Journal of Geophysical Research: Solid Earth, 130(5), e2024JB030256. https://doi.org/ 10.1029/ 2024JB030 256.

[8] Lin, L.-C. J., Chuang, R. Y., & Nishimura, T. (2025). Exploring Coulomb stress changes on active structures in Taiwan inferred from decadal GNSS observations. Earth, Planets and Space, 77, Article 88. https://doi.org/ 10.1186/ s40623-025-02095-7.

[9] Das, R., Meneses, C., & Wang, H. (2025). Seismic and GNSS strain-based probabilistic seismic hazard evaluation for northern Chile using DAS Magnitude Scale. Geoenvironmental Disasters, 12, Article 1. https://doi.org/10.1186/s40677-024-00261-2.

[10] Nishimura, T. (2018). A trial application of geodetic data for inland fault assessment—Coulomb stress changes estimated from GNSS surface displacements. Journal of Disaster Research, 13(3), 489–495. https://doi.org/ 10.20965/ jdr. 2018. p0489.